High-cell-density production of adeno-associated viral vector serotype 6 by triple transfection in suspension HEK293 cell cultures

Pablo Moço[1], Xingge Xu[1], and Amine Kamen[1]

[1]McGill University

February 2, 2023

Abstract

The use of adeno-associated viruses (AAV) as vectors for gene and cell therapy has risen considerably in recent years. Consequently, the amount of AAV vectors required during the validation and clinical trials has also increased. AAV serotype 6 (AAV6) is well-documented for its efficiency in transducing different cell types and has been successfully used in gene and cell therapy protocols. However, the number of vectors required to effectively deliver the transgene to one single cell has been estimated at 106 viral genomes (VG). Overall, this means that large-scale production of AAV6 is needed. Suspension cell-based platforms are currently limited to low-cell-density productions, hindering the potential of this production process to increase yields. Here, we investigate the improvement of the production of AAV6 at higher cell densities. The production was performed by transient transfection of HEK293SF cells. When the plasmid DNA is provided on a cell basis, the production can be carried out at medium cell density without effects on cell-specific titer or particle functionality, resulting in titers above 1010 VG/mL. Medium supplementation alleviated the cell density effect, in terms of VG/cell, at high-cell-density productions. On the other hand, the cell-specific functional titer was not maintained, and further studies are necessary to understand the observed limitations. The medium-cell-density production method reported here lays the foundation for large-scale process operations, potentially solving the current vector shortage in AAV manufacturing.

Research Article

High-cell-density production of adeno-associated viral vector serotype 6 by triple transfection in suspension HEK293 cell cultures

Pablo D. Moço[1]

Xingge Xu[1]

Amine A. Kamen[1]

[1]Department of Bioengineering, McGill University, Montreal, Canada

Correspondence: Dr. Amine Kamen, Department of Bioengineering, McGill University, 3480 University Street | McConnell Engineering Building, Room 363, Montreal, QC, H3A 0E9 Canada.

E-mail : amine.kamen@mcgill.ca

Keywords: Bioprocess engineering, Bioprocess development, Cell culture, Mammalian cells, Viruses.

Abbreviations: AAV , adeno-associated virus; **AAV6** , AAV serotype 6; **CDE** , cell density effect; **CSVY** , cell-specific viral yield; **ETU** , enhanced transducing units;**FDA** , U. S. Food and Drug Administration; **GFP** , green fluorescent protein; **GOI** , gene of interest; **HCD** , high cell density; **LCD** , low cell density, **MCD** , medium cell density; **PEI** , polyethylenimine; **VG** , viral genomes.

ABSTRACT

The use of adeno-associated viruses (AAV) as vectors for gene and cell therapy has risen considerably in recent years. Consequently, the amount of AAV vectors required during the validation and clinical trials has also increased. AAV serotype 6 (AAV6) is well-documented for its efficiency in transducing different cell types and has been successfully used in gene and cell therapy protocols. However, the number of vectors required to effectively deliver the transgene to one single cell has been estimated at 10^6 viral genomes (VG). Overall, this means that large-scale production of AAV6 is needed. Suspension cell-based platforms are currently limited to low-cell-density productions, hindering the potential of this production process to increase yields. Here, we investigate the improvement of the production of AAV6 at higher cell densities. The production was performed by transient transfection of HEK293SF cells. When the plasmid DNA is provided on a cell basis, the production can be carried out at medium cell density without effects on cell-specific titer or particle functionality, resulting in titers above 10^{10} VG/mL. Medium supplementation alleviated the cell density effect, in terms of VG/cell, at high-cell-density productions. On the other hand, the cell-specific functional titer was not maintained, and further studies are necessary to understand the observed limitations. The medium-cell-density production method reported here lays the foundation for large-scale process operations, potentially solving the current vector shortage in AAV manufacturing.

INTRODUCTION

Adeno-associated viruses (AAVs) are small, 25-nm-wide, icosahedral, non-enveloped viruses with a 4.7-kb-long single-stranded DNA genome belonging to the family *Parvoviridae* [1]. AAVs are non-pathogenic and replication-defective [2], depending on co-infection with helper viruses, such as Adenovirus or Herpes Simplex virus. First discovered from stocks of adenovirus in the 1960s [2, 3], AAVs have recently become a critical gene delivery vector for treating diseases. Glybera was the first AAV-based gene therapy drug approved in 2012 by the European Medicines Agency [4]. The US Food and Drug Administration (FDA) approved 2 AAV-based gene therapy drugs, Luxturna, in 2017 [5] and, Zolgesma, in 2019 [6].

To this date, based on phylogenetic analysis, 13 different serotypes and more than 100 variants of AAV have been identified [2, 3, 7-14]. Due to heterogeneity in capsid proteins, each serotype exhibits a distinct tropism and ability to transduce different cell types [15]. Serotype 6 has a wide range of target cells and has been shown to successfully transduce cells in the central nervous system [16], human prostate, breast, and liver cancer cells [17], melanocytes [18], skeletal muscle [19-21], heart [22-24], lung [25], and the eye [26]. Recently, AAV6 gained popularity due to its ability to transduce lymphocytes [27-29] and its use for generating Chimeric Antigen Receptor T cells [30-36].

The number of therapeutic AAV applications being investigated is steadily increasing, with more than 300 completed or ongoing clinical trials [37]. These applications require large amounts of AAV vectors to validate pre-clinical animal studies and clinical trials. Reported doses can reach up to 7.5×10^{15} VG for targeted delivery and up to 1.5×10^{17} VG for systemic delivery [38]. This large requirement in the number of viral vectors implies that an improvement in current production methods is necessary. This is especially true for AAV serotype 6, which requires up to 10^6 VG/cell during the transduction of T cells [27]. Recombinant AAV is produced by replacing the viral genes, *Rep* and *Cap* , with the gene of interest (GOI). Mammalian cells are transiently transfected with a GOI cassette flanked by the inverted terminal repeats, a plasmid carrying the *Rep* and *Cap* functions, and a third plasmid encoding the helper functions [39-42]. The transient transfection is generally done using the cost-effective cationic polymer, Polyethylenimine (PEI) [43]. However, adherent cell cultures are not deemed viable for AAV production at scales that exceed 10^{15} total VGs, making them unsuitable for late-phase clinical trials and commercial applications of these viral vectors [44]. The use of HEK293 cells in suspension for producing AAV vectors was first described in 2006 [45]. Despite many efforts in optimizing production, large-scale production of AAV vectors is considered a bottleneck in their implementation as a widespread type of viral vector for gene therapy and cell therapy [46], mainly because current HEK293-based production is done at low cell densities [45, 47-51]. Limiting the production of viral vectors to lower cell densities hinders the potential of this production process to be intensified [52]. On the other hand, the production of viral vectors at higher cell densities tends to be limited by the widely reported cell density effect (CDE), which results in diminished transfection and productivity [53-55]. In this

manuscript, we demonstrate that the production of AAV serotype 6 via transient transfection is not limited to low-cell-density cultures.

MATERIAL AND METHODS

Cell line and culture

HEK293SF cells were maintained in serum-free suspension cultures at 37°C, 5% CO_2, and 75% relative humidity in a shaker incubator (Infors, Switzerland) at 135 rpm speed of agitation or specified otherwise. The basal maintenance and production medium was HyCell TransFx-H (Cytiva Life Sciences, USA) supplemented with 0.1% w/v of Kolliphor P188 (Sigma-Aldrich, USA) and 4 mM GlutaMAX (Gibco, USA). GlutaMAX was replaced by 6 mM L-Glutamine (Gibco, USA) for experiments in which nutrients and metabolites were analyzed. The supplemented medium was prepared by adding either glucose for a final concentration of 7.2 g/L or 15% (v/v) Cell Boost 5 (Cytiva Life Sciences, USA) to achieve a similar glucose concentration.

Low- and medium-cell-density cultures (1 and 4 $\times$ 10^6cells/mL, respectively, at the time of transfection - TOT) were done in 125-mL polycarbonate shake flasks (TriForest, USA) with a working volume of 25 mL. High-cell-density (10×10^6 cells/mL at TOT) transfection was performed in 50-mL TubeSpin bioreactors (TPP, Switzerland) with a working volume of 10 mL and 180 rpm. For achieving and maintaining high cell densities, from 48 hours post-seeding, a perfusion-like mode of operation was followed with medium exchange of 1 vessel volume per day (VVD) both before and after transfection, where cells were centrifuged and resuspended in fresh medium.

The bioreactor production was performed in a 3-L vessel (Applikon Biotechnology, The Netherlands) equipped with a double marine impeller, a pH sensor, a temperature sensor, a dissolved oxygen (DO) concentration sensor, a micro sparger with 100-nm pore size, and a capacitance probe for monitoring of cell culture characteristics, such as cell growth. The pH, temperature, and DO parameters were set at 7.15 $\pm$ 0.05, 37°C, and 40% oxygen saturation, respectively. The HEK293SF cells from shake flasks were inoculated into the bioreactor at 4 $\times$ 10^6cells/mL in a fresh culture medium. The transfection was conducted immediately after cell inoculation with plasmid delivered on a cell basis (1 µg/10^6 cells).

Plasmids

The following plasmids were used to produce adeno-associated viral vectors: (1) pAdDeltaF6 was a gift from James M. Wilson (Addgene plasmid #112867; http://n2t.net/addgene:112867; RRID:Addgene_112867), (2) pRep2Cap6 (provided by Dr. Samulski, University of North Carolina, USA), (3) pAAV-CAG-GFP was a gift from Edward Boyden (Addgene plasmid #37825; http://n2t.net/addgene:37825; RRID:Addgene_37825) and (4) pX601-AAV-saCas9-sgRNA, modified from pX601-AAV-CMV::NLS-SaCas9-NLS-3xHA-bGHpA;U6::BsaI-sgRNA, a gift from Feng Zhang (Addgene plasmid #61591; http://n2t.net/addgene:61591; RRID:Addgene_61591).

Transient transfection

Recombinant AAV6 particles expressing GFP driven by the CAG promoter were produced via triple transient transfection of HEK293SF cells as previously described [56]. In brief, the transgene plasmid pAAV-CAG-GFP, the plasmid pRep2Cap6, and the helper plasmid pAdDeltaF6 were co-transfected into HEK293SF cells in a ratio of 1:1:1 after complexation with 25-KDa linear polyethylenimine (PEI, Polysciences, USA) at a ratio of 1:2 (DNA:PEI). Plasmid DNA and PEI were diluted separately in HyCell TransFx-H in a volume corresponding to 2.5% of the volume of cells to be transfected. For experiments where the DNA was delivered on a volumetric basis, 1 µg of plasmid was added per millilitre of cell culture. For delivering DNA on a cell basis, 1 µg of plasmid was added per million viable cells. Diluted DNA and PEI were mixed and incubated at room temperature for 15 minutes. The DNA-PEI cocktail was then added to the cells.

Determination of transfection efficiency

For evaluation of transfection efficiency, cells were collected 24 hours post-transduction and fixed with a solution of 2% paraformaldehyde. Cells were analyzed using a BD Accuri C6 flow cytometer (BD Biosciences,

USA), and EGFP expression was analyzed using BD Accuri C6 Plus Analysis Software (BD Biosciences, USA).

Harvest of produced viral vectors

Viral particles were harvested from the cell culture broth as previously described [47, 56]. Briefly, the cells were harvested and lysed by adding a 10X Lysis Buffer (20 mM $MgCl_2$, 1% Triton X-100 in 500 mM Tris-buffered solution). Benzonase was added to a final concentration of 5 U/mL to digest host-cell DNA and unpacked virus DNA. After 1 hour of incubation at 37°C with agitation, $MgSO_4$was added to a final concentration of 37.5 mM to prevent AAV aggregation and binding to cellular components. After 30 minutes of incubation at 37°C with agitation, the lysate was clarified via centrifugation at 10,000 × g for 15 minutes. The clarified viral lysate was stored in a -80°C freezer.

AAV genome quantification by droplet digital PCR

Genome-containing viral particles were titrated via ddPCR [57]. Viral DNA from samples was extracted using a High Pure Viral Nucleic Acid Extraction kit (Roche Diagnostics, Switzerland). The following primers targeting the transgene were used: EGFP, 5'-CTGCTGCCCGACAACCAC-3' (forward) and 5'-TCACGAACTCCAGCAGGAC-3' (reverse); SaCas9, 5'-GGCCAGATTCAGGATGTGCT-3' (forward) and 5'- CATCATCCCCAGAAGCGTGT-3' (reverse). The primers were purchased from Integrated DNA Technologies (USA). The thermocycling temperature programming for EGFP was: preincubation at 95°C/15 min for denaturation. 40 cycles of 94°C/30 s, 53°C/30 s and 72°C/1 min, and final extension at 72°C for 5 min. For SaCas9 was: preincubation at 95°C/15 min for denaturation. 40 cycles of 94°C/30 s, 60°C/1 min and 72°C/30 s, and final extension at 72°C for 5 min. The plates were scanned on a QX100 droplet reader (Bio-Rad, USA), and the analysis was carried out with QuantaSoft software (Bio-Rad, USA). Quantification was performed as previously described [58]. Cell-specific viral yield (CSVY) was determined by dividing the titer by the cell density at the time of transfection.

Functional virus titer via gene transfer assay

Suspension-adapted HEK293SF cells were transduced with serial dilutions of AAV6-GFP and co-infected with an E1, E3-deleted adenovirus serotype 5 ([?]E_1E_3Ad5) at an MOI of 5 infectious particles/cell. At 24 hours post-transduction, the cells were harvested and fixed in 2% paraformaldehyde at 4degC for 30 min. Cells were analyzed using a BD Accuri C6 flow cytometer (BD Biosciences, USA), and EGFP expression was analyzed using BD Accuri C6 Plus Analysis Software (BD Biosciences, USA). The linear range of quantification was established between 2%–20% of GFP-positive cells [59].

Analysis of medium nutrients and metabolites

Culture samples were collected every 24 h, centrifuged for removal of cell pellet, and the supernatant was analyzed in a BioProfile FLEX2 Analyzer (Nova Biomedical, USA) to determine the following nutrients and metabolites: glutamine, glutamic acid, glucose, lactate, and ammonium.

Statistical analysis

Results are expressed as mean +- standard deviation. Student's t-test was used to measure the statistical significance between two groups. One-way ANOVA followed by Dunnett's post-hoc test was used to measure the statistical difference between three or more groups. $P< 0.05$ was considered to indicate a statistically significant difference. Asterisks are used to indicate P values as follows: *, $P < 0.05$; **, $P < 0.01$; ***,$P < 0.005$, ****, $P < 0.0005$.

RESULTS

Effect of plasmid DNA availability on AAV production at low cell densities

In the present study, we investigated the improvement of AAV6 production via transient transfection of suspension-adapted HEK293SF cells by increasing cell density. The standard AAV production in our laboratory is conducted via transfection at low cell density with 1 µg of plasmid DNA per mL. First, we assessed

if plasmid DNA availability played an important role during production in an increased cell density. We compared the AAV6 yield from productions at 1 and 2 million cells per mL. During transfection, plasmid DNA was delivered either on a volumetric basis (1 μg/mL) or a cell basis (1 μg/10^6 cells). PEI concentration for all experiments was set at 2 μg per μg of plasmid DNA. Viral vectors were harvested 48 hours post-transfection (hpt) to determine viral yield in terms of genome-containing particles (viral genomes, VG). The cell density and viability profiles during AAV production are shown in Figure 1A. Lower transduction efficiencies were observed in both productions at 2 million cells per mL compared to the control (Figure 1B). A 2.4-fold increase in viral titer was observed in the transfection of 2 million cells per mL when DNA was supplied on a cell basis (5.4×10^9 VG/mL), resulting in a better-than-linear increase of viral titer when compared to the standard production (2.2×10^9 VG/mL) (Figure 1C). Productions at 2 million cells per mL showed the highest cell-specific viral yield (CSVY) only when DNA was supplied on a cell basis (approximately 3100 VG/cell). The delivery of DNA as 1 μg/mL in the transfection of 2 million cells per mL caused a reduction in the CSVY to only 900 VG/cell, resulting in a volumetric yield of only 1.8×10^9 VG/mL.

Cell-specific production maintained at a medium cell density

The next step was to evaluate the viral vector production at a medium cell density (MCD, 4×10^6 cells/mL at the time of transfection). Again, the cells were transfected with plasmids on either a volumetric or cell basis and the viral titer VG/mL was assessed every 24 hours. Figure 2A shows the cell density and viability profiles during AAV production at low and medium cell densities. A drop in the transfection efficiency was observed even when a higher amount of DNA was supplied (Figure 2C). However, as previously observed, this lower transduction efficiency did not impact viral titer (Figure 2B, DNA delivered on a cell basis). Similar to what was observed in the transfection of 2 million cells per mL, the titer of the MCD production with DNA delivered on a cell basis was 3.8 times the control, reaching 8.6×10^9VG/mL (Figure 2B). DNA delivery on a volumetric basis resulted in 4.9×10^9 VG/mL (a 2.2-fold increase from the control). When DNA is supplied on a cell basis, the CSVY was maintained at around 2,000 VG/cell. On the other hand, volumetric delivery of DNA resulted in a decrease to 1,200 VG/cell (Figure 2B). The functional viral titers (enhanced transduction units (ETU)/mL) are summarized in Figure 2D. An increase in cell density resulted in a rise of functional titer by 2.5-3.9 times, depending on the harvest time. At 48 hpt, no statistically significant difference ($P = 0.4261$) was observed in the ratio VG/ETU between low- and medium-cell-density production with 1 μg of DNA per million cells (Figure 2E).

The cell density effect is observed at higher densities

To study if cell-based delivery of DNA would be enough to prevent the cell density effect at a high-cell-density (HCD) production, we evaluated AAV6 production at 10 million cells per mL. A perfusion-like mode of operation was devised in 50-mL TubeSpin bioreactors to achieve the desired cell density. A working volume of 10 mL and medium exchange of 1 vessel volume per day (VVD) were set. The medium exchange started 24 hours after the seeding of the cells and was maintained past the transfection to keep providing fresh nutrients to the cells. Cells were transfected at a density of 10×10^6 cells/mL, with plasmid DNA delivered on a cell basis, and viral titer was assessed every 24 hours. A low-cell-density (LCD) control was also prepared in similar vessels. As expected, the transduction of the high cell-density production was lower than the control (Figure 3A). Cell densities and volumetric titers during AAV6 productions are shown in Figure 3B. AAV6 yield peaked at 72 hpt, and the HCD production resulted in 9.3×10^9 VG/mL, a 4.6-fold increase compared to the LCD control. Even though the yield was higher than the control, this result shows that the titer does not increase linearly with the increase in cell density at the time of transfection. This difference becomes even more evident at the cell-specific level. At 72 hpt, the LCD batch control yielded an average of 1,600 VG/cell, while the HCD perfusion yielded less than 1,000 VG/cell (Figure 5B).

Medium supplementation improves cell-specific production of genome-containing particles

Nutrients and cell metabolites were analyzed during the production of AAV6 at low and high cell densities in TubeSpin bioreactors. Even though the levels of metabolites (lactate and ammonium) would be maintained low, and levels of glutamine and glutamic acid were kept constant by the medium exchange, a significant

drop in glucose concentration was observed (Figures 4A and B). At 48 hpt, glucose concentration was 3.2 g/L for LCD, while for HCD, as low as 1.8 g/L. Two other HCD productions were performed to evaluate the effect of medium supplementation. This time, the medium was supplemented with either glucose at a final concentration of 7.2 g/L or 15% Cell Boost 5, which resulted in a similar concentration of glucose between LCD and HCD production at their lowest points (Figure 4B).

Figure 5A shows the cell density and viability profiles during AAV production at high cell density with basal and supplemented media, and Figure 5B shows the transduction efficiency 24 hours post-transfection. Medium supplementation with Cell Boost 5 resulted in a higher growth rate after transfection, with cell density reaching 25.5×10^6 cells/mL 96 hpt, while cells in basal medium reached up to 20.4×10^6 cells/mL. Cells cultured in the glucose-supplemented medium showed a slower growth rate, resulting in the transfection being done one day later compared to the medium supplemented with Cell Boost 5. At 72 hpt, when compared to the use of the basal medium, the use of supplementation resulted in increased volumetric titer (1.4- and 1.6-fold increase for glucose and Cell Boost 5, respectively) and a significant improvement of cell-specific titer (1.8-fold increase for Cell Boost 5) (Figure 5C).

Medium supplementation alleviated the observed cell density effect in the HCD production, resulting in CSVY similar to those in the LCD control, leading to an almost 10-fold increase in viral titer. There was an increase in functional titer when HCD production was supplemented. Cell-specific functional titer also increases depending on the supplementation, but it was 2 times inferior compared to the LCD (Figure 6A). The VG/ETU ratio for LCD production was 34.4, while for HCD, it reached 79.9 when the medium was supplemented with Cell Boost 5 (Figure 6B).

Validation of medium-cell-density production at bioreactor scale

Since the MCD production resulted in a significant improvement in titer and no loss in functionality, we decided to evaluate the scalability of this process. For that, we conducted the production in a 3-L bioreactor, where the cells were seeded at 4×10^6 cells/mL in fresh medium and were immediately transfected with plasmids delivered on a cell basis. Whole broth culture was sampled at 8-16h intervals. A satellite culture, with a volume of around 25 mL taken from the bioreactor post-transfection, was evaluated in parallel in a shake flask (Figure S1). At 24 hpt, a transfection efficiency of 36.9% was observed, similar to the production in shake flasks (33.8%, Figure 2C). Figure 7 shows cellular and production kinetics in the bioreactor, demonstrating that MCD production is feasible at a bioreactor scale. Low-cell-density 3-L bioreactor productions previously completed in our laboratory were used as control. In these LCD runs, AAV6 vectors packaging a genome without fluorescent marker were produced; thus, it was impractical to assess their functional titer. Cell density in the MCD bioreactor reached its maximum at 59 hpt with 9.5×10^6 viable cells/mL. Vector production peaked around 60 hpt with a titer of 5.9×10^{10} VG/mL, a ˜4-fold increase compared to control bioreactors (Figure 7C). At this point, the cell-specific titer was around 15,000 VG/cell, a similar value to the one obtained by LCD production in bioreactors (Figure 7D). Regarding the functional titer, the bioreactor yielded 7.8×10^9 ETU/mL 48 hours post-transfection (Figure 7E). As a result, the VG/ETU ratio was as low as 4.6 at 48 hpt, plateauing around 10 at subsequent time points (Figure 7F).

DISCUSSION

In Figure 1, we observe that plasmid DNA availability plays an essential role in the maintenance of VG titer when cell density at the time of transfection is increased from 1 to 2 million cells per mL. In low-cell-density transient transfection, plasmid DNA is usually delivered on a volumetric basis [45, 47-50]. Like our study, Grieger, Soltys and Samulski [48] also observed a titer increase during production when cell density and plasmid concentration were doubled. The need for a higher plasmid DNA concentration was also observed for productions at 4×10^6 cells/mL (medium cell density, MCD). A 4-fold increase in the number of cells at the time of transfection resulted in an almost linear increase in viral titer (VG/mL) only when plasmid DNA was delivered per million cells (Figure 2B). Moreover, the cell-specific yield was maintained during MCD production, with plasmid DNA concentration maintained on a per-cell basis (Figure 2B). Yields between 1,500 and 3,000 VG/cell were obtained, similar to those reported by Chahal, Schulze, Tran, Montes and

Kamen [47]. The improvement in titer was also observed for functional particles (ETU). The functional titer of the MCD production with plasmid DNA delivered on a cell basis was maintained constant (Figure 2D), resulting in a difference of up to 3.9 times compared to the LCD control at 96 hpt. At LCD, the slight decrease in transducing units, but not in genome-containing particles, could be explained by the loss in functionality of the viral vectors. AAV vectors are thermally stable, but their transduction efficiency decreases when maintained at 37°C and as the pH decreases [60]. Extending the culture to 96 hpt can decrease intracellular and extracellular pH due to the accumulation of metabolites, such as ammonia and lactate [61, 62].

The VG/ETU ratio measures viral functionality, showing the proportion of genome-containing viruses competent to transduce a target cell. At 48 hpt, the MCD production had a mean VG/ETU ratio of 67.1 (Figure 2E). Although this value is higher than reported in the literature [47, 48], there was no statistically significant difference from our LCD control. As shown in Figure 7, the production of AAV6 at medium cell density was successfully performed at a 3-L bioreactor. The cells were inoculated into the bioreactor in fresh medium at the desired cell density of 4×10^6 cells/mL to prevent detrimental effects from the spent medium. At larger scales, this could be achieved, for example, by medium exchange using Tangential Flow Depth Filtration (TFDF) as a cell retention device [63, 64]. This bioreactor production resulted in 30- and 7.5-fold increase in VG/mL and VG/cell titers, respectively, compared to previously reported production at a similar scale [47]. Surprisingly, the viral vector yield on the bioreactor was around 10-fold higher than the small-scale satellite culture. Similarly, the LCD bioreactor production also showed a higher yield than the small-scale experiments. This enhanced production in the bioreactors could be associated with better-regulated culture conditions, such as dissolved oxygen and pH. Again, no loss in functional titer was observed, with a maximum value of 7.8×10^9 ETU/mL achieved 48 hours post-transfection and a VG/ETU ratio of 4.6 (Figure 7D and E). These results show an improvement from previous reports [47, 48].

When productions were conducted at cell densities other than 1×10^6 cell/mL, the transfection efficiency, measured by the expression of the transgene 24 hours post-transfection, decreased to about 30% independently of the cell density (Figure 1B, Figure 2C, and Figure 3A). However, the percentage of cells expressing the transgene did not correlate directly with production efficiency. Others observed this same phenomenon during the production of viral-like particles via transient transfection of HEK293SF suspension cells [65]. Hildinger, Baldi, Stettler and Wurm [66] concluded that the transfection efficiency reduction resulted from DNA being provided on a volumetric basis. However, increasing the plasmid DNA availability in our study did not significantly improve transduction efficiency (Figure 1B, Figure 2C, and Figure 3A), as measured by the detection of the product of one of the three plasmids, which corroborates previous findings [47]. Increased energetic demand is reported to occur at higher cell densities and to allow recovery from transfection, an event known to be cytotoxic [67]. Transfection efficiency did not improve during production in a perfusion-like mode, even when the medium was supplemented (Figure 5B). The transfection efficiency was even lower at a higher glucose concentration. Lavado-García, Jorge, Cervera, Vázquez and Gòdia [67] partially explained the low transfection efficiency as a result of downregulated pathways involved in lipid biosynthesis and nuclear transportation of intracellular proteins. The transfection step, per se, is a known bottleneck in the production of AAV vectors. A recent study from our group showed that the proportion of cells that produce viral particles is as low as 7%, despite high transduction efficiency [68].

Recently, the improvement of AAV8 production at high-cell density with a medium exchange strategy was reported [64]. Conversely, the cell density effect was confirmed during our high-cell-density productions (Figures 3B and 5). CDE refers to the diminished production at high cell densities resulting from decreased cell-specific productivity [55, 69]. This effect has been previously documented for the generation of AAV using other production systems, such as insect cells [53, 59, 70-72]. During production, 25 to 30% of the AVV6 vectors are released in the supernatant [47]. Because of the high cell density and the elevated shaking speed to properly oxygenate the bioreactors used, it is possible that the cells were under increased sheer stress and could have released more vectors into the supernatant, which were removed during the medium exchange. This could explain the sudden drop in viral titer at 96 hpt in the HCD production (Figure 3B), which is not expected since AAV vectors are considered very stable at a wide range of temperatures [60, 73]. The same drop, however, was not observed when the medium was supplemented (Figure 5C).

The cell density effect is thought to occur mainly due to metabolic limitations caused by low concentrations of nutrients or the accumulation of inhibitory metabolites [53, 55, 74]. During the production at HCD, a perfusion-like mode was employed to provide enough nutrients to support high cell density and remove inhibitory metabolites; however, the conditions selected were insufficient to prevent the CDE (Figure 3). The glucose level dropped significantly at HCD, even though the medium was fully exchanged daily. For that reason, the basal medium, HyCell TransFx-H, which contains around 6 g/L of glucose, was supplemented with either glucose or Cells Boost 5. The amount of supplement added was based on the cell-specific consumption rate of glucose so that a minimum of 2 g/L of glucose was available at any given time [75], mimicking the observed glucose concentrations in the LCD productions. Medium supplementation with glucose alone did not restore the cell-specific productivity of AAV6 (Figure 5C). The CDE was alleviated, and the cell-specific yield (VG/cell) was restored only when a medium supplemented with 15% Cell Boost 5 was used (Figure 5C), indicating that other critical nutrients were limiting viral vector yield. Besides glucose, other components of the Cell Boost 5 supplement are thought to contribute to alleviating the CDE. While producing adenoviral vectors using the HEK293SF cells, Shen, Voyer, Tom and Kamen [76] emphasized that the composition of the medium used is crucial to support high yields at HCD. However, the complexity of culture media and supplements, such as Cell Boost 5, which can contain hundreds of different components at variable concentrations, complicates the understanding of individual nutrients' effect on viral vector productions [55]. An optimized cell culture medium to produce AAV vectors could improve titers and vector quality, as seen and suggested for other viral vectors [61, 67, 75, 76].

As discussed above, supplementing the medium with Cell Boost 5 alleviated the cell density effect in terms of genome-containing particles; however, the same was not observed for functional particles. Whereas there was an increase in functional yield when the medium was supplemented, the cell-specific functional titer (ETU/cell) was not fully maintained, resulting in higher VG/ETU ratios compared to the LCD control (Figure 6). One possible explanation is the misassembly of the viral capsid, which contains a stoichiometry of 1:1:10 (VP1:VP2:VP3). If this proportion is altered, the efficacy of the AAV to deliver the transgene decreases [77]. Due to nuclear localization signals, the VP1 and VP2 proteins play a crucial role in transduction, specifically in nuclear transportation [78]. The N-terminus of VP1 also contains a phospholipase A2 domain responsible for viral escape from the endosome [79-82]. Our results highlight the importance of assessing viral transduction efficacy by measuring biologically active vectors [83] as part of optimizing AAV vector production. This measurement is sometimes overlooked by authors [49, 51], even though the quality attributes of a viral vector, including functional titer, are an essential part of the potency tests recommended by the FDA [84].

In summary, we demonstrated that it is possible to produce AAV6 via triple transient transfection at medium cell density without losing cell-specific productivity or functional titer. For that, the plasmid DNA must be provided on a cell basis. Our medium-cell-density productions achieved titers at the order of 10^{10} VG/mL of crude lysate. The yields obtained by this method represent a significant increase compared to a well-established production protocol [47]. The medium-cell-density method for AAV vector production described in this manuscript was shown to be efficient at a 3-L bioreactor scale. It could be used as the foundation for large-scale production processes, potentially contributing to solving the current vector shortage in AAV manufacturing. The cell density effect could be alleviated at a higher cell density, resulting in similar cell-specific productivity (VG/cell) when a perfusion-like operation was conducted with a supplemented medium. However, the cell-specific functional productivity (ETU/cell) was reduced, highlighting the importance of evaluating both viral genomes and transducing units during bioprocess optimization. Further research is necessary to fully understand how the cell density effect results in reduced functional titer and how to alleviate it fully.

ACKNOWLEDGMENT

PDM is financially supported by a fellowship from the Faculty of Engineering at McGill University and a doctoral scholarship from the Fonds de Recherche du Québec – Santé (FRQS). XX is financially supported by a doctoral scholarship from Fonds de Recherche du Québec – Nature et technologies (FRQNT). AAK is

partially funded through Canada Research Chair CRC-240394. The funding sources were not involved in the study design, the collection, analysis and interpretation of data, the writing of the report or the decision to submit the article for publication. The authors would like to thank Cristina Silva for her support.

DATA AVAILABILITY STATEMENT:

The data that support the findings of this study are available from the corresponding author upon reasonable request.

AUTHOR CONTRIBUITIONS

Conceptualization: PDM, AAK; Investigation: PDM, XX; Formal analysis: PDM; Writing - original draft: PDM; Writing – review & editing: PDM, XX, AAK; Supervision: AAK, Funding acquisition: AAK

DECLARATION OF COMPETING INTEREST

The authors declare that they have no known competing financial interests or personal relationships that could have appeared to influence the work reported in this paper.

REFERENCES

[1] Georg-Fries, B., Biederlack, S., Wolf, J., zur Hausen, H., Analysis of proteins, helper dependence, and seroepidemiology of a new human parvovirus. *Virology* **1984** , *134* , 64-71.

[2] Atchison, R. W., Casto, B. C., Hammon, W. M., Adenovirus-Associated Defective Virus Particles. *Science***1965** , *149* , 754-756.

[3] Hoggan, M. D., Blacklow, N. R., Rowe, W. P., Studies of small DNA viruses found in various adenovirus preparations: physical, biological, and immunological characteristics. *Proc. Natl. Acad. Sci. USA* **1966** , *55* , 1467-1474.

[4] European Medicines Agency, Assessment Report: Glybera.**2012** .

[5] U. S. Food and Drug Administration, Luxturna BL 125610/0 Approval Letter. **2017** .

[6] U. S. Food and Drug Administration, Zolgesma BL 125694/0 Approval Letter. **2019** .

[7] Parks, W. P., Melnick, J. L., Rongey, R., Mayor, H. D., Physical Assay and Growth Cycle Studies of a Defective Adeno-Satellite Virus.*J. Virol.* **1967** , *1* , 171-180.

[8] Bantel-Schaal, U., Zur Hausen, H., Characterization of the DNA of a defective human parvovirus isolated from a genital site. *Virology* **1984** , *134* , 52-63.

[9] Rutledge, E. A., Halbert, C. L., Russell, D. W., Infectious Clones and Vectors Derived from Adeno-Associated Virus (AAV) Serotypes Other Than AAV Type 2. *J. Virol.* **1998** , *72* , 309-319.

[10] Gao, G. P., Alvira, M. R., Wang, L., Calcedo, R., Johnston, J., Wilson, J. M., Novel adeno-associated viruses from rhesus monkeys as vectors for human gene therapy. *Proc. Natl. Acad. Sci. USA***2002** , *99* , 11854-11859.

[11] Gao, G., Vandenberghe, L. H., Alvira, M. R., Lu, Y., Calcedo, R., Zhou, X., Wilson, J. M., Clades of Adeno-Associated Viruses Are Widely Disseminated in Human Tissues. *J. Virol.* **2004** ,*78* , 6381-6388.

[12] Mori, S., Wang, L., Takeuchi, T., Kanda, T., Two novel adeno-associated viruses from cynomolgus monkey: pseudotyping characterization of capsid protein. *Virology* **2004** ,*330* , 375-383.

[13] Schmidt, M., Voutetakis, A., Afione, S., Zheng, C., Mandikian, D., Chiorini, J. A., Adeno-Associated Virus Type 12 (AAV12): a Novel AAV Serotype with Sialic Acid- and Heparan Sulfate Proteoglycan-Independent Transduction Activity. *J. Virol.* **2008** , *82* , 1399-1406.

[14] Schmidt, M., Govindasamy, L., Afione, S., Kaludov, N., Agbandje-McKenna, M., Chiorini, J. A., Molecular characterization of the heparin-dependent transduction domain on the capsid of a novel adeno-associated virus isolate, AAV(VR-942). *J. Virol.***2008** , *82* , 8911-8916.

[15] Srivastava, A., In vivo tissue-tropism of adeno-associated viral vectors. *Curr. Opin. Virol.* **2016** , *21* , 75-80.

[16] Schober, A. L., Gagarkin, D. A., Chen, Y., Gao, G., Jacobson, L., Mongin, A. A., Recombinant Adeno-Associated Virus Serotype 6 (rAAV6) Potently and Preferentially Transduces Rat Astrocytes In vitro and In vivo. *Front. Cell. Neurosci.* **2016** , *10* , 262.

[17] Sayroo, R., Nolasco, D., Yin, Z., Colon-Cortes, Y., Pandya, M., Ling, C., Aslanidi, G., Development of novel AAV serotype 6 based vectors with selective tropism for human cancer cells. *Gene Ther.***2016** , *23* , 18-25.

[18] Sheppard, H. M., Ussher, J. E., Verdon, D., Chen, J., Taylor, J. A., Dunbar, P. R., Recombinant Adeno-Associated Virus Serotype 6 Efficiently Transduces Primary Human Melanocytes. *PLoS One***2013** , *8* , e62753.

[19] Blankinship, M. J., Gregorevic, P., Allen, J. M., Harper, S. Q., Harper, H., Halbert, C. L., Miller, D. A., Chamberlain, J. S., Efficient transduction of skeletal muscle using vectors based on adeno-associated virus serotype 6. *Mol. Ther.* **2004** ,*10* , 671-678.

[20] Wang, Z., Kuhr, C. S., Allen, J. M., Blankinship, M., Gregorevic, P., Chamberlain, J. S., Tapscott, S. J., Storb, R., Sustained AAV-mediated Dystrophin Expression in a Canine Model of Duchenne Muscular Dystrophy with a Brief Course of Immunosuppression.*Mol. Ther.* **2007** , *15* , 1160-1166.

[21] Qiao, C., Zhang, W., Yuan, Z., Shin, J. H., Li, J., Jayandharan, G. R., Zhong, L., Srivastava, A., Xiao, X., Duan, D., Adeno-associated virus serotype 6 capsid tyrosine-to-phenylalanine mutations improve gene transfer to skeletal muscle. *Hum. Gene Ther.* **2010** , *21* , 1343-1348.

[22] Palomeque, J., Chemaly, E. R., Colosi, P., Wellman, J. A., Zhou, S., Del Monte, F., Hajjar, R. J., Efficiency of eight different AAV serotypes in transducing rat myocardium in vivo. *Gene Ther.***2007** , *14* , 989-997.

[23] Raake, P. W., Hinkel, R., Müller, S., Delker, S., Kreuzpointner, R., Kupatt, C., Katus, H. A., Kleinschmidt, J. A., Boekstegers, P., Müller, O. J., Cardio-specific long-term gene expression in a porcine model after selective pressure-regulated retroinfusion of adeno-associated viral (AAV) vectors. *Gene Ther.***2008** , *15* , 12-17.

[24] White, J. D., Thesier, D. M., Swain, J. B. D., Katz, M. G., Tomasulo, C., Henderson, A., Wang, L., Yarnall, C., Fargnoli, A., Sumaroka, M., Isidro, A., Petrov, M., Holt, D., Nolen-Walston, R., Koch, W. J., Stedman, H. H., Rabinowitz, J., Bridges, C. R., Myocardial gene delivery using molecular cardiac surgery with recombinant adeno-associated virus vectors in vivo. *Gene Ther.* **2011** ,*18* , 546-552.

[25] van Lieshout, L. P., Domm, J. M., Rindler, T. N., Frost, K. L., Sorensen, D. L., Medina, S. J., Booth, S. A., Bridges, J. P., Wootton, S. K., A Novel Triple-Mutant AAV6 Capsid Induces Rapid and Potent Transgene Expression in the Muscle and Respiratory Tract of Mice.*Mol. Ther. Methods Clin. Dev.* **2018** , *9* , 323-329.

[26] Sharma, A., Ghosh, A., Hansen, E. T., Newman, J. M., Mohan, R. R., Transduction efficiency of AAV 2/6, 2/8 and 2/9 vectors for delivering genes in human corneal fibroblasts. *Brain Res. Bull.***2010** , *81* , 273-278.

[27] Wang, J., DeClercq, J. J., Hayward, S. B., Li, P. W., Shivak, D. A., Gregory, P. D., Lee, G., Holmes, M. C., Highly efficient homology-driven genome editing in human T cells by combining zinc-finger nuclease mRNA and AAV6 donor delivery. *Nucleic Acids Res.***2015** , *44* , e30.

[28] Rogers, G. L., Huang, C., Clark, R. D. E., Seclén, E., Chen, H.-Y., Cannon, P. M., Optimization of AAV6 transduction enhances site-specific genome editing of primary human lymphocytes. *Mol. Ther. Methods Clin. Dev.* **2021** , *23* , 198-209.

[29] Nawaz, W., Huang, B., Xu, S., Li, Y., Zhu, L., Yiqiao, H., Wu, Z., Wu, X., AAV-mediated in vivo CAR gene therapy for targeting human T-cell leukemia. *Blood Cancer J.* **2021** , *11* , 119.

[30] Sather, B. D., Romano Ibarra, G. S., Sommer, K., Curinga, G., Hale, M., Khan, I. F., Singh, S., Song, Y., Gwiazda, K., Sahni, J., Jarjour, J., Astrakhan, A., Wagner, T. A., Scharenberg, A. M., Rawlings, D. J., Efficient modification of CCR5 in primary human hematopoietic cells using a megaTAL nuclease and AAV donor template. *Sci. Transl. Med.* **2015** , *7* , 307ra156.

[31] Hale, M., Lee, B., Honaker, Y., Leung, W. H., Grier, A. E., Jacobs, H. M., Sommer, K., Sahni, J., Jackson, S. W., Scharenberg, A. M., Astrakhan, A., Rawlings, D. J., Homology-Directed Recombination for Enhanced Engineering of Chimeric Antigen Receptor T Cells. *Mol. Ther. Methods Clin. Dev.* **2017** , *4* , 192-203.

[32] MacLeod, D. T., Antony, J., Martin, A. J., Moser, R. J., Hekele, A., Wetzel, K. J., Brown, A. E., Triggiano, M. A., Hux, J. A., Pham, C. D., Bartsevich, V. V., Turner, C. A., Lape, J., Kirkland, S., Beard, C. W., Smith, J., Hirsch, M. L., Nicholson, M. G., Jantz, D., McCreedy, B., Integration of a CD19 CAR into the TCR Alpha Chain Locus Streamlines Production of Allogeneic Gene-Edited CAR T Cells. *Mol. Ther.* **2017** , *25* , 949-961.

[33] Eyquem, J., Mansilla-Soto, J., Giavridis, T., van der Stegen, S. J., Hamieh, M., Cunanan, K. M., Odak, A., Gonen, M., Sadelain, M., Targeting a CAR to the TRAC locus with CRISPR/Cas9 enhances tumour rejection. *Nature* **2017** , *543* , 113-117.

[34] Dai, X., Park, J. J., Du, Y., Kim, H. R., Wang, G., Errami, Y., Chen, S., One-step generation of modular CAR-T cells with AAV-Cpf1.*Nat. Methods* **2019** , *16* , 247-254.

[35] Moço, P. D., Aharony, N., Kamen, A., Adeno-Associated Viral Vectors for Homology-Directed Generation of CAR-T Cells.*Biotechnol. J.* **2020** , *15* , 1900286.

[36] Naeimi Kararoudi, M., Likhite, S., Elmas, E., Yamamoto, K., Schwartz, M., Sorathia, K., de Souza Fernandes Pereira, M., Sezgin, Y., Devine, R. D., Lyberger, J. M., Behbehani, G. K., Chakravarti, N., Moriarity, B. S., Meyer, K., Lee, D. A., Optimization and validation of CAR transduction into human primary NK cells using CRISPR and AAV.*Cell Rep. Methods* **2022** .

[37] ClinicalTrials.gov, **2022** .

[38] Au, H. K. E., Isalan, M., Mielcarek, M., Gene Therapy Advances: A Meta-Analysis of AAV Usage in Clinical Settings. *Front. Med.***2021** , *8* , 809118.

[39] Grimm, D., Kern, A., Rittner, K., Kleinschmidt, J. A., Novel tools for production and purification of recombinant adenoassociated virus vectors. *Hum. Gene Ther.* **1998** , *9* , 2745-2760.

[40] Xiao, X., Li, J., Samulski, R. J., Production of high-titer recombinant adeno-associated virus vectors in the absence of helper adenovirus. *J. Virol.* **1998** , *72* , 2224-2232.

[41] Collaco, R. F., Cao, X., Trempe, J. P., A helper virus-free packaging system for recombinant adeno-associated virus vectors.*Gene* **1999** , *238* , 397-405.

[42] Matsushita, T., Elliger, S., Elliger, C., Podsakoff, G., Villarreal, L., Kurtzman, G., Iwaki, Y., Colosi, P., Adeno-associated virus vectors can be efficiently produced without helper virus.*Gene Ther.* **1998** , *5* , 938-945.

[43] Wright, J. F., Transient Transfection Methods for Clinical Adeno-Associated Viral Vector Production. *Hum. Gene Ther.***2009** , *20* , 698-706.

[44] Salabarria, S. M., Nair, J., Clement, N., Smith, B. K., Raben, N., Fuller, D. D., Byrne, B. J., Corti, M., Advancements in AAV-mediated Gene Therapy for Pompe Disease. *J. Neuromuscul. Dis.***2020** , *7* , 15-31.

[45] Park, J. Y., Lim, B. P., Lee, K., Kim, Y. G., Jo, E. C., Scalable production of adeno-associated virus type 2 vectors via suspension transfection. *Biotechnol. Bioeng.* **2006** ,*94* , 416-430.

[46] Smith, J., Grieger, J., Samulski, R. J., Overcoming Bottlenecks in AAV Manufacturing for Gene Therapy. *Cell Gene Ther. Insights***2018** , *4* , 815-825.

[47] Chahal, P. S., Schulze, E., Tran, R., Montes, J., Kamen, A. A., Production of adeno-associated virus (AAV) serotypes by transient transfection of HEK293 cell suspension cultures for gene delivery.*J. Virol. Methods* **2014** , *196* , 163-173.

[48] Grieger, J. C., Soltys, S. M., Samulski, R. J., Production of Recombinant Adeno-associated Virus Vectors Using Suspension HEK293 Cells and Continuous Harvest of Vector From the Culture Media for GMP FIX and FLT1 Clinical Vector. *Mol. Ther.* **2016** , *24* , 287-297.

[49] Blessing, D., Vachey, G., Pythoud, C., Rey, M., Padrun, V., Wurm, F. M., Schneider, B. L., Deglon, N., Scalable Production of AAV Vectors in Orbitally Shaken HEK293 Cells. *Mol. Ther. Methods Clin. Dev.* **2019** , *13* , 14-26.

[50] Zhao, H., Lee, K. J., Daris, M., Lin, Y., Wolfe, T., Sheng, J., Plewa, C., Wang, S., Meisen, W. H., Creation of a High-Yield AAV Vector Production Platform in Suspension Cells Using a Design-of-Experiment Approach. *Mol. Ther. Methods Clin. Dev.* **2020** , *18* , 312-320.

[51] Guan, J.-S., Chen, K., Si, Y., Kim, T., Zhou, Z., Kim, S., Zhou, L., Liu, X., Process Improvement of Adeno-Associated Virus Production. *Front. Chem. Eng.* **2022** , *4* .

[52] Rajendra, Y., Balasubramanian, S., Hacker, D. L., Large-Scale Transient Transfection of Chinese Hamster Ovary Cells in Suspension,*Methods Mol. Biol.* , Springer New York **2017** , pp. 45-55.

[53] Bernal, V., Carinhas, N., Yokomizo, A. Y., Carrondo, M. J., Alves, P. M., Cell density effect in the baculovirus-insect cells system: a quantitative analysis of energetic metabolism.*Biotechnol. Bioeng.* **2009** , *104* , 162-180.

[54] Le Ru, A., Jacob, D., Transfiguracion, J., Ansorge, S., Henry, O., Kamen, A. A., Scalable production of influenza virus in HEK-293 cells for efficient vaccine manufacturing. *Vaccine* **2010** ,*28* , 3661-3671.

[55] Petiot, E., Cuperlovic-Culf, M., Shen, C. F., Kamen, A., Influence of HEK293 metabolism on the production of viral vectors and vaccine. *Vaccine* **2015** , *33* , 5974-5981.

[56] Joshi, P. R. H., Bernier, A., Moco, P. D., Schrag, J., Chahal, P. S., Kamen, A., Development of a Scalable and Robust Anion-Exchange Chromatographic Method for Enriched Recombinant Adeno-Associated Virus Preparations in Genome Containing Vector Capsids of Serotypes- 5, 6, 8, and 9. *Mol. Ther. Methods Clin. Dev.* **2021** , *21* , 341-356.

[57] Lock, M., Alvira, M. R., Chen, S. J., Wilson, J. M., Absolute determination of single-stranded and self-complementary adeno-associated viral vector genome titers by droplet digital PCR. *Hum. Gene Ther. Methods* **2014** , *25* , 115-125.

[58] Furuta-Hanawa, B., Yamaguchi, T., Uchida, E., Two-Dimensional Droplet Digital PCR as a Tool for Titration and Integrity Evaluation of Recombinant Adeno-Associated Viral Vectors. *Hum. Gene Ther. Methods* **2019** , *30* , 127-136.

[59] Joshi, P. R. H., Cervera, L., Ahmed, I., Kondratov, O., Zolotukhin, S., Schrag, J., Chahal, P. S., Kamen, A. A., Achieving High-Yield Production of Functional AAV5 Gene Delivery Vectors via Fedbatch in an Insect Cell-One Baculovirus System. *Mol. Ther. Methods Clin. Dev.* **2019** , *13* , 279-289.

[60] Lins-Austin, B., Patel, S., Mietzsch, M., Brooke, D., Bennett, A., Venkatakrishnan, B., Van Vliet, K., Smith, A. N., Long, J. R., McKenna, R., Potter, M., Byrne, B., Boye, S. L., Bothner, B., Heilbronn, R., Agbandje-Mckenna, M., Adeno-Associated Virus (AAV) Capsid Stability and Liposome Remodeling During Endo/Lysosomal pH Trafficking. *Viruses* **2020** , *12* , 668.

[61] Ferreira, T. B., Carrondo, M. J., Alves, P. M., Effect of ammonia production on intracellular pH: Consequent effect on adenovirus vector production. *J. Biotechnol.* **2007** , *129* , 433-438.

[62] Patel, S. D., Papoutsakis, E. T., Winter, J. N., Miller, W. M., The lactate issue revisited: novel feeding protocols to examine inhibition of cell proliferation and glucose metabolism in hematopoietic cell cultures. *Biotechnol. Prog.* **2000** , *16* , 885-892.

[63] Tran, M. Y., Kamen, A. A., Production of Lentiviral Vectors Using a HEK-293 Producer Cell Line and Advanced Perfusion Processing. *Front. Bioeng. Biotechnol.* **2022** , *10* , 887716.

[64] Mendes, J. P., Fernandes, B., Pineda, E., Kudugunti, S., Bransby, M., Gantier, R., Peixoto, C., Alves, P. M., Roldao, A., Silva, R. J. S., AAV process intensification by perfusion bioreaction and integrated clarification. *Front. Bioeng. Biotechnol.* **2022** , *10* , 1020174.

[65] Cervera, L., Gutierrez-Granados, S., Martinez, M., Blanco, J., Godia, F., Segura, M. M., Generation of HIV-1 Gag VLPs by transient transfection of HEK 293 suspension cell cultures using an optimized animal-derived component free medium. *J. Biotechnol.* **2013** , *166* , 152-165.

[66] Hildinger, M., Baldi, L., Stettler, M., Wurm, F. M., High-titer, serum-free production of adeno-associated virus vectors by polyethyleneimine-mediated plasmid transfection in mammalian suspension cells. *Biotechnol. Lett* **2007** , *29* , 1713-1721.

[67] Lavado-Garcia, J., Jorge, I., Cervera, L., Vazquez, J., Godia, F., Multiplexed Quantitative Proteomic Analysis of HEK293 Provides Insights into Molecular Changes Associated with the Cell Density Effect, Transient Transfection, and Virus-Like Particle Production. *J. Proteome Res.* **2020** , *19* , 1085-1099.

[68] Dash, S., Sharon, D. M., Mullick, A., Kamen, A. A., Only a small fraction of cells produce assembled capsids during transfection-based manufacturing of adeno-associated virus vectors. *Biotechnol. Bioeng.* **2022** .

[69] Joshi, P. R. H., Venereo-Sanchez, A., Chahal, P. S., Kamen, A. A., Advancements in molecular design and bioprocessing of recombinant adeno-associated virus gene delivery vectors using the insect-cell baculovirus expression platform. *Biotechnol. J.* **2021** ,*16* , 2000021.

[70] Elias, C. B., Zeiser, A., Bedard, C., Kamen, A. A., Enhanced growth of sf-9 cells to a maximum density of 5.2 x 107 cells per mL and production of β-galactosidase at high cell density by fed batch culture. *Biotechnol. Bioeng.* **2000** , *68* , 381-388.

[71] Meghrous, J., Aucoin, M. G., Jacob, D., Chahal, P. S., Arcand, N., Kamen, A. A., Production of recombinant adeno-associated viral vectors using a baculovirus/insect cell suspension culture system: from shake flasks to a 20-L bioreactor. *Biotechnol. Prog.* **2005** , *21* , 154-160.

[72] Mena, J. A., Aucoin, M. G., Montes, J., Chahal, P. S., Kamen, A. A., Improving adeno-associated vector yield in high density insect cell cultures. *J. Gene Med.* **2010** , *12* , 157-167.

[73] Bennett, A., Patel, S., Mietzsch, M., Jose, A., Lins-Austin, B., Yu, J. C., Bothner, B., McKenna, R., Agbandje-Mckenna, M., Thermal Stability as a Determinant of AAV Serotype Identity. *Mol. Ther. Methods Clin. Dev.* **2017** , *6* , 171-182.

[74] Bereiter-Hahn, J., Munnich, A., Woiteneck, P., Dependence of energy metabolism on the density of cells in culture. *Cell Struct. Funct.* **1998** , *23* , 85-93.

[75] Martinez, V., Gerdtzen, Z. P., Andrews, B. A., Asenjo, J. A., Viral vectors for the treatment of alcoholism: Use of metabolic flux analysis for cell cultivation and vector production. *Metab. Eng.* **2010** , *12* ,

129-137.

[76] Shen, C. F., Voyer, R., Tom, R., Kamen, A., Reassessing culture media and critical metabolites that affect adenovirus production.*Biotechnol. Prog.* **2009** , *26* , NA-NA.

[77] Bosma, B., Du Plessis, F., Ehlert, E., Nijmeijer, B., De Haan, M., Petry, H., Lubelski, J., Optimization of viral protein ratios for production of rAAV serotype 5 in the baculovirus system. *Gene Ther.* **2018** , *25* , 415-424.

[78] Grieger, J. C., Snowdy, S., Samulski, R. J., Separate basic region motifs within the adeno-associated virus capsid proteins are essential for infectivity and assembly. *J. Virol.* **2006** ,*80* , 5199-5210.

[79] Girod, A., Wobus, C. E., Zádori, Z., Ried, M., Leike, K., Tijssen, P., Kleinschmidt, J. A., Hallek, M., The VP1 capsid protein of adeno-associated virus type 2 is carrying a phospholipase A2 domain required for virus infectivity. *J. Gen. Virol.* **2002** ,*83* , 973-978.

[80] Sonntag, F., Bleker, S., Leuchs, B., Fischer, R., Kleinschmidt, J. A., Adeno-associated virus type 2 capsids with externalized VP1/VP2 trafficking domains are generated prior to passage through the cytoplasm and are maintained until uncoating occurs in the nucleus. *J. Virol.* **2006** , *80* , 11040-11054.

[81] Venkatakrishnan, B., Yarbrough, J., Domsic, J., Bennett, A., Bothner, B., Kozyreva, O. G., Samulski, R. J., Muzyczka, N., McKenna, R., Agbandje-McKenna, M., Structure and dynamics of adeno-associated virus serotype 1 VP1-unique N-terminal domain and its role in capsid trafficking. *J. Virol.* **2013** , *87* , 4974-4984.

[82] Stahnke, S., Lux, K., Uhrig, S., Kreppel, F., Hosel, M., Coutelle, O., Ogris, M., Hallek, M., Buning, H., Intrinsic phospholipase A2 activity of adeno-associated virus is involved in endosomal escape of incoming particles. *Virology* **2011** , *409* , 77-83.

[83] Francois, A., Bouzelha, M., Lecomte, E., Broucque, F., Penaud-Budloo, M., Adjali, O., Moullier, P., Blouin, V., Ayuso, E., Accurate Titration of Infectious AAV Particles Requires Measurement of Biologically Active Vector Genomes and Suitable Controls. *Mol. Ther. Methods Clin. Dev.* **2018** , *10* , 223-236.

[84] U. S. Food and Drug Administration, Guidance for Industry: Potency Tests for Cellular and Gene Therapy Products. **2011** .

FIGURE LEGENDS

Figure 1. Production of AAV6 via triple transient transfection at low cell densities. Cells were transfected at 1 or 2 million cells per mL, and plasmid DNA was delivered on a volumetric basis (VB - 1 μg/mL) or cell basis (CB - 1 $\mu g/10^6$ cells). A) Cell growth kinetics and viability. Black arrows indicate the time of transfection, and dashed arrows indicate the time of viral harvest. B) Transfection efficiency is described as the percentage of cells expressing the transgene (GFP) 24 hours post-transfection. C) Volumetric (VG/mL) and cell-specific viral yields (VG/cell). Ctrl: transfection at 1×10^6 cells/mL; 2M: at 2×10^6cells/mL. Values represent mean ± standard deviation (n=3). ** $P< 0.01$, * $P < 0.05$, by ANOVA followed by Dunnett's test.

Figure 2. Production of AAV6 via triple transient transfection at medium cell densities. Cells were transfected at low cell density (LCD – 1×10^6 cells/mL) as control or at medium cell density (MCD – 4×10^6 cells/mL). Plasmid DNA was delivered on a volumetric basis (VB - 1 μg/mL) or cell basis (CB - 1 $\mu g/10^6$ cells). A) Cell growth kinetics and viability. B) Volumetric (VG/mL) and cell-specific viral yields (VG/cell). Time expressed in hours post-transfection (hpt). C) Transfection efficiency is described as the percentage of cells expressing the transgene (GFP) 24 hpt D) Functional titer (enhanced transducing units (ETU)/mL). E) Ratio between the genomic titer and functional titer (VG/ETU) 48 hpt. Values represent mean ± standard deviation (n=2). **** $P < 0.0001$, *** $P < 0.001$, by ANOVA followed by Dunnett's test and Student's T-test.

Figure 3. Production of AAV6 via triple transient transfection at high cell density. A) transfection efficiency is described as the percentage of cells expressing the transgene (GFP) 24 hours post-transfection. B) Cell growth kinetics (*) and volumetric viral yield (). Cells were transfected at low cell density (LCD – 1 x 10^6

cells/mL) as control or at high cell density (HCD – 10 x 10^6 cells/mL). Plasmid DNA was delivered on a cell basis (1 µg/10^6 cells). Values represent mean ± standard deviation (n=3). *** P < 0.001, by Student's T test.

Figure 4. Metabolic profile of production of AAV6 via triple transient transfection at high cell density. Cells were transfected at low cell density (LCD – 1 × 10^6 cells/mL) as control or at high cell density (HCD – 10 × 10^6 cells/mL). Plasmid DNA was delivered on a cell basis (1 µg/10^6 cells). A) Nutrient and metabolite concentration for production at low and high cell densities using basal or supplemented medium (7.2 g/L final glucose concentration or 15% Cell Boost 5). The dashed line represents the time of transfection. B) Concentration of glucose for productions at low and high cell densities. Time expressed as hours post-transfection (hpt). Values represent mean ± standard deviation (n=3).

Figure 5. Effect of medium supplementation on the production of AAV6. HyCell TransFx-H (basal medium) was supplemented with glucose (7.2 g/L final concentration) or with 15% Cell Boost 5. A) Cell growth kinetics and viability. Black arrows indicate the time of transfection. B) Transfection efficiency is described as the percentage of cells expressing the transgene (GFP) 24 hours post-transfection (hpt). C) Volumetric (VG/mL) and cell-specific viral yields (VG/cell) of low cell-density control and high cell-density productions with basal and supplemented media. Values represent mean ± standard deviation (n=3).

Figure 6. Production of AAV6 at different cell densities. A) Functional titer (ETU/mL) and cell-specific functional titer (ETU/mL) at 72 hpt. B) Ratio between volumetric and functional titer at 72 hpt. LCD: low cell density control; HCD: high cell density. Values represent mean ± standard deviation (n=3). $^{**}P < 0.01$, $^{*}\ P < 0.05$, by ANOVA followed by Dunnett's test.

Figure 7. Bioreactor production of AAV6 at medium cell density. Cells were transfected at 4 million cells per mL (medium cell density, MCD), and plasmid DNA was delivered on a cell basis (1 µg/10^6cells). Low-cell-density (LCD, 1 × 10^6 cell/mL) bioreactor productions shown as control. Time indicated as hours post-transfection (hpt). A) Bioreactor control chart. B) Cell growth kinetics and viability. C) Volumetric titer (VG/mL). D) Cell-specific viral yield (VG/cell). E) Functional titer (ETU/mL). F) Ratio between volumetric and functional titer (VG/ETU). Values represent mean ± standard deviation (n=1 for MCD; n=2 for LCD).

Figure S1. Satellite culture from bioreactor production of AAV6 at medium cell density. Cells were transfected at 4 million cells per mL (medium cell density, MCD), and plasmid DNA was delivered on a cell basis (1 µg/10^6 cells). Time indicated as hours post-transfection (hpt). A) Cell growth kinetics and viability. B) Volumetric titer (VG/mL). C) Cell-specific viral yield (VG/cell). D) Functional titer (ETU/mL). E) Ratio between volumetric and functional titer (VG/ETU). n=1.

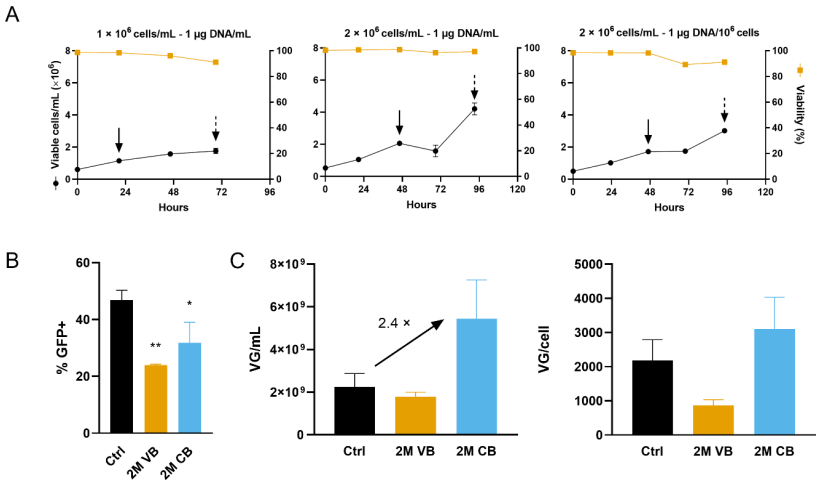

Figure 1. Production of AAV6 via triple transient transfection at low cell densities. Cells were transfected at 1 or 2 million cells per mL, and plasmid DNA was delivered on a volumetric basis (VB - 1 μg/mL) or cell basis (CB - 1 μg/10^6 cells). A) Cell growth kinetics and viability. Black arrows indicate the time of transfection, and dashed arrows indicate the time of viral harvest. B) Transfection efficiency is described as the percentage of cells expressing the transgene (GFP) 24 hours post-transfection. C) Volumetric (VG/mL) and cell-specific viral yields (VG/cell). Ctrl: transfection at 1 × 10^6 cells/mL; 2M: at 2 × 10^6cells/mL. Values represent mean ± standard deviation (n=3). ** $P< 0.01$, * $P < 0.05$, by ANOVA followed by Dunnett's test.

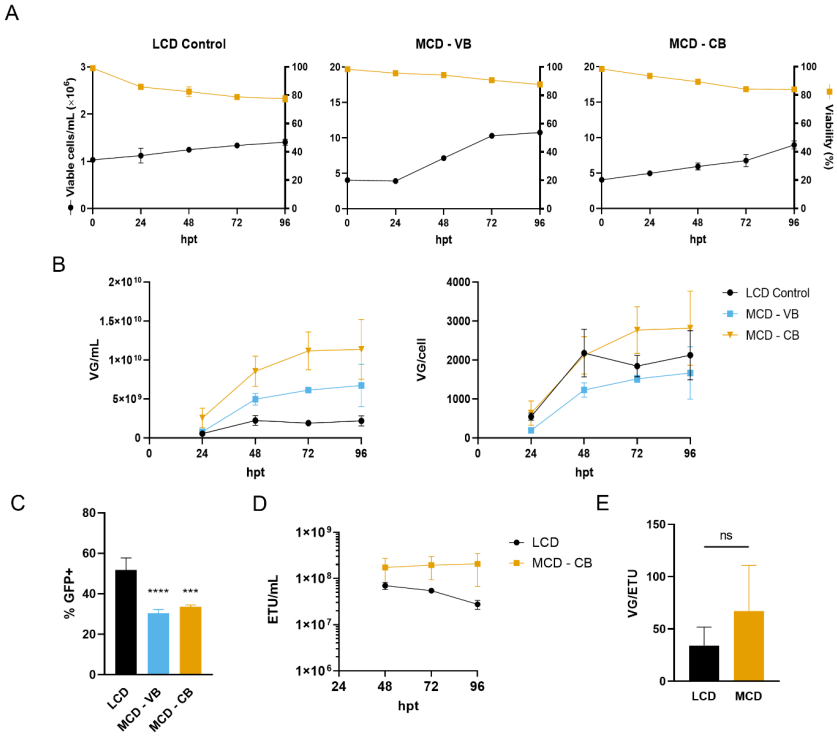

Figure 2. Production of AAV6 via triple transient transfection at medium cell densities. Cells were transfected at low cell density (LCD – 1 × 10^6 cells/mL) as control or at medium cell density (MCD – 4 × 10^6 cells/mL). Plasmid DNA was delivered on a volumetric basis (VB - 1 μg/mL) or cell basis (CB - 1 μg/10^6 cells). A) Cell growth kinetics and viability. B) Volumetric (VG/mL) and cell-specific viral yields (VG/cell). Time expressed in hours post-transfection (hpt). C) Transfection efficiency is described as the percentage of cells expressing the transgene (GFP) 24 hpt D) Functional titer (enhanced transducing units (ETU)/mL). E) Ratio between the genomic titer and functional titer (VG/ETU) 48 hpt. Values represent mean ± standard deviation (n=2). **** P < 0.0001, *** P < 0.001, by ANOVA followed by Dunnett's test and Student's T-test.

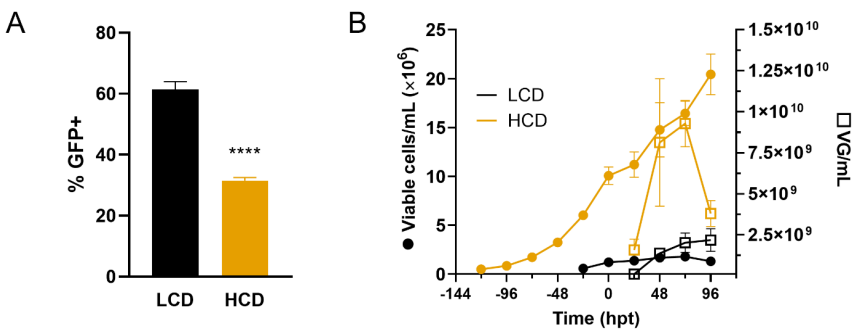

Figure 3. Production of AAV6 via triple transient transfection at high cell density. A) transfection efficiency is described as the percentage of cells expressing the transgene (GFP) 24 hours post-transfection. B) Cell growth kinetics (*) and volumetric viral yield (). Cells were transfected at low cell density (LCD – 1×10^6 cells/mL) as control or at high cell density (HCD – 10×10^6 cells/mL). Plasmid DNA was delivered on a cell basis (1 µg/10^6 cells). Values represent mean ± standard deviation (n=3). *** $P < 0.001$, by Student's T test.

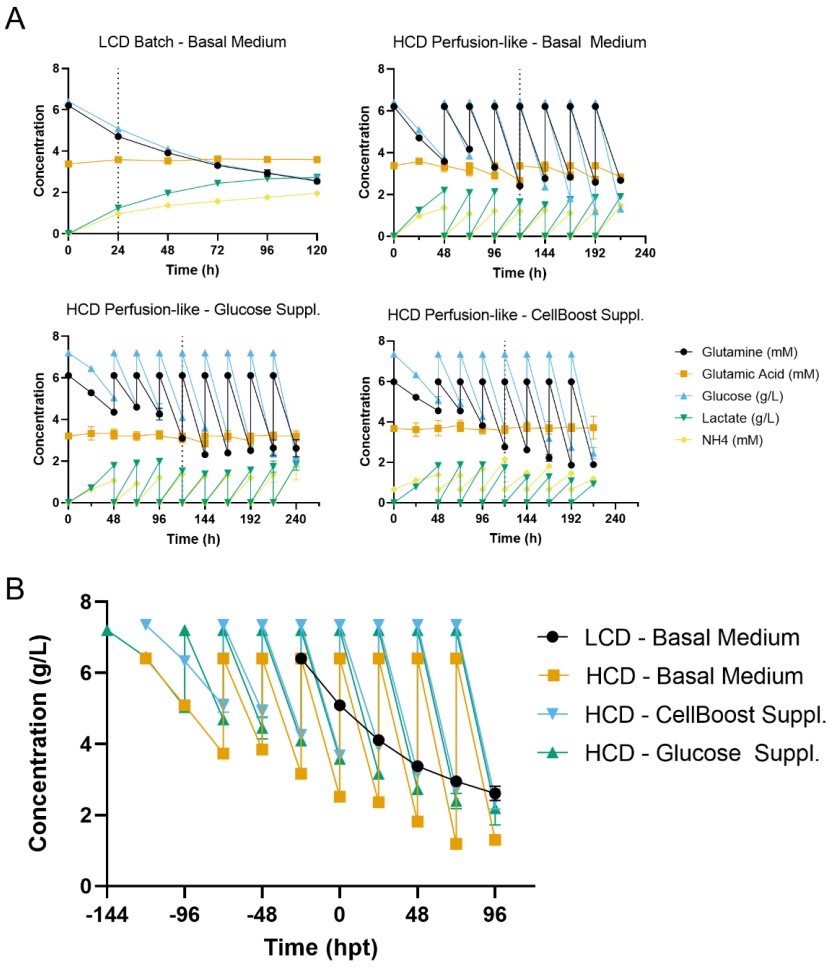

Figure 4. Metabolic profile of production of AAV6 via triple transient transfection at high cell density. Cells were transfected at low cell density (LCD – 1×10^6 cells/mL) as control or at high cell density (HCD – 10×10^6 cells/mL). Plasmid DNA was delivered on a cell basis (1 μg/10^6cells). A) Nutrient and metabolite concentration for production at low and high cell densities using basal or supplemented medium (7.2 g/L final glucose concentration or 15% Cell Boost 5). The dashed line represents the time of transfection. B) Concentration of glucose for productions at low and high cell densities. Time expressed as hours post-transfection (hpt). Values represent mean ± standard deviation (n=3).

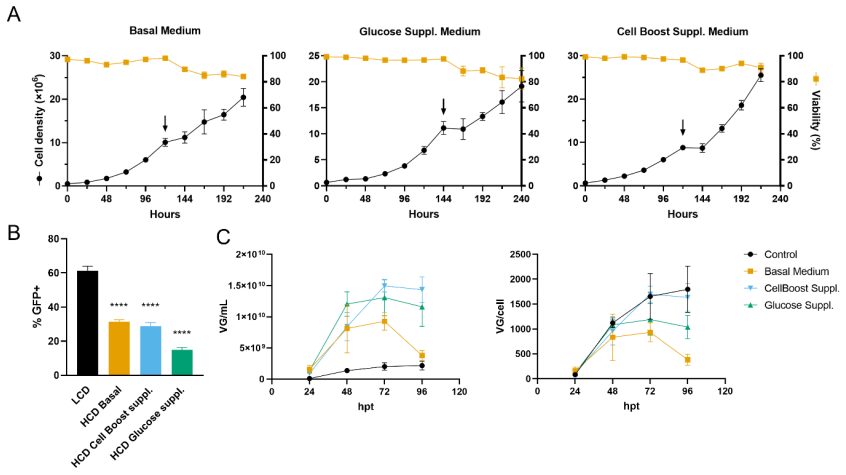

Figure 5. Effect of medium supplementation on the production of AAV6. HyCell TransFx-H (basal medium) was supplemented with glucose (7.2 g/L final concentration) or with 15% Cell Boost 5. A) Cell growth kinetics and viability. Black arrows indicate the time of transfection. B) Transfection efficiency is described as the percentage of cells expressing the transgene (GFP) 24 hours post-transfection (hpt). C) Volumetric (VG/mL) and cell-specific viral yields (VG/cell) of low cell-density control and high cell-density productions with basal and supplemented media. Values represent mean ± standard deviation (n=3).

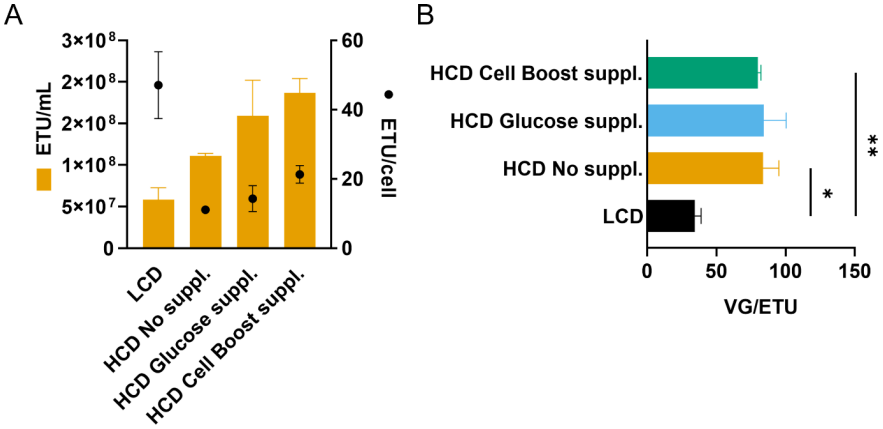

Figure 6. Production of AAV6 at different cell densities. A) Functional titer (ETU/mL) and cell-specific functional titer (ETU/mL) at 72 hpt. B) Ratio between volumetric and functional titer at 72 hpt. LCD: low cell density control; HCD: high cell density. Values represent mean ± standard deviation (n=3). ** $P < 0.01$, * $P < 0.05$, by ANOVA followed by Dunnett's test.

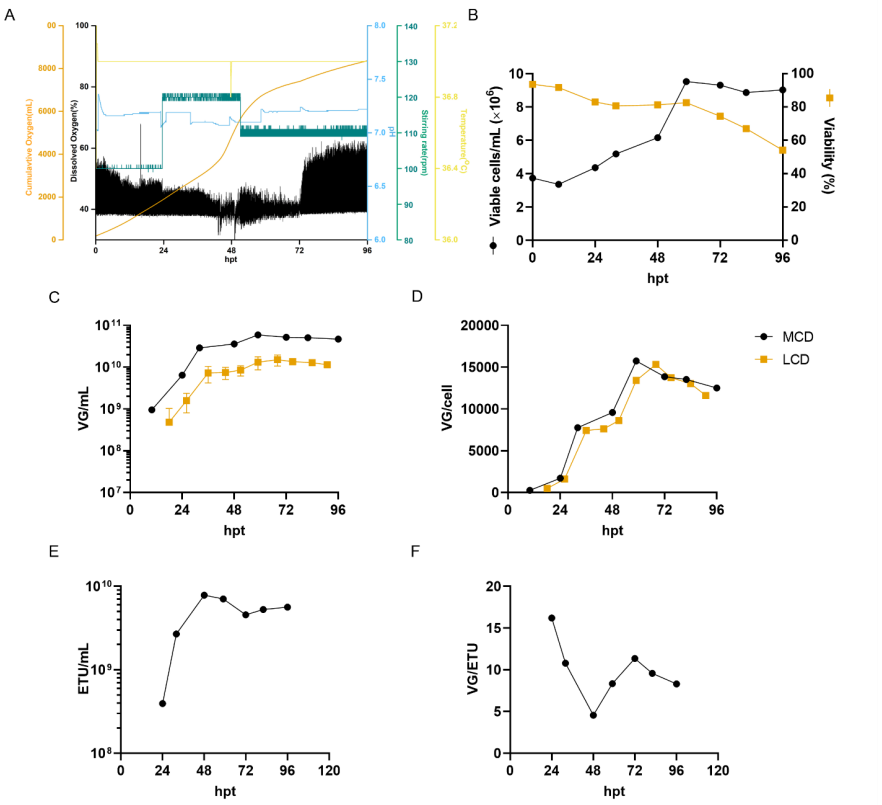

Figure 7. Bioreactor production of AAV6 at medium cell density. Cells were transfected at 4 million cells per mL (medium cell density, MCD), and plasmid DNA was delivered on a cell basis (1 μg/10^6 cells). Low-cell-density (LCD, 1 × 10^6 cell/mL) bioreactor productions shown as control. Time indicated as hours post-transfection (hpt). A) Bioreactor control chart. B) Cell growth kinetics and viability. C) Volumetric titer (VG/mL). D) Cell-specific viral yield (VG/cell). E) Functional titer (ETU/mL). F) Ratio between volumetric and functional titer (VG/ETU). Values represent mean ± standard deviation (n=1 for MCD; n=2 for LCD).

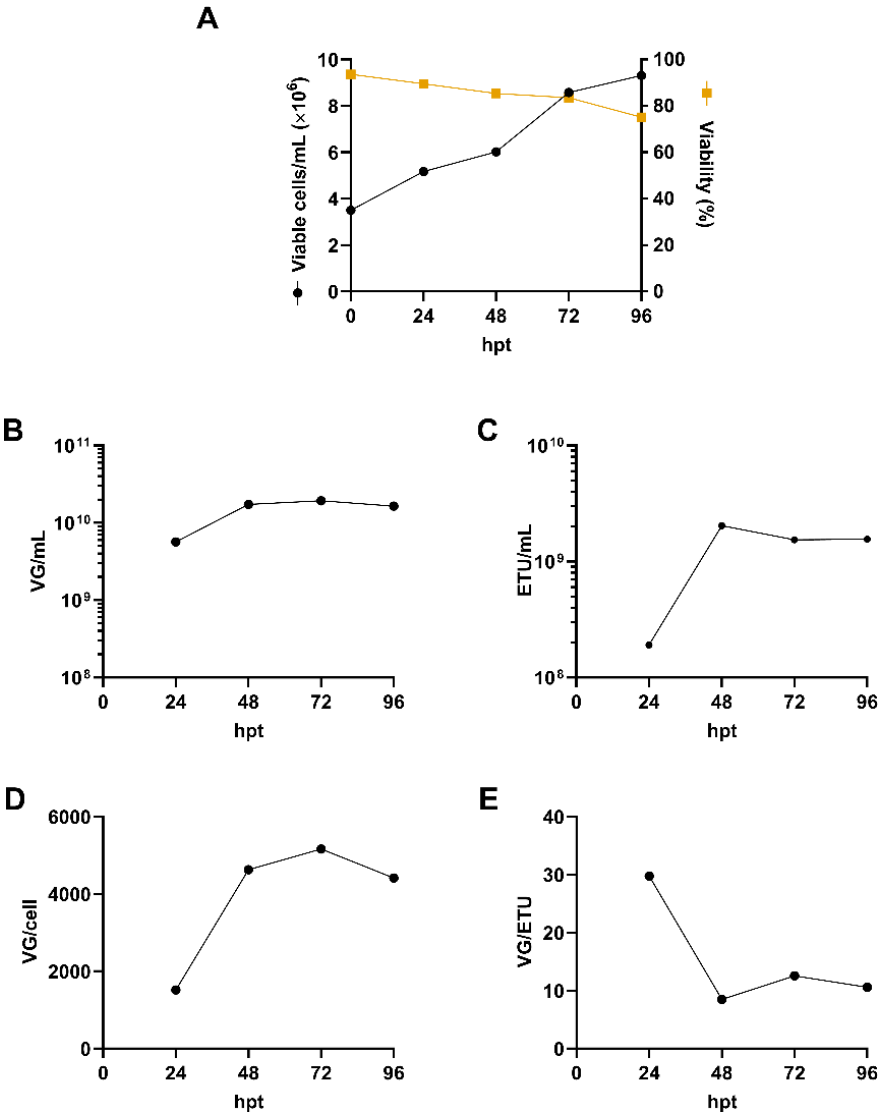

Figure S1. Satellite culture from bioreactor production of AAV6 at medium cell density. Cells were transfected at 4 million cells per mL (medium cell density, MCD), and plasmid DNA was delivered on a cell basis (1 μg/10^6 cells). Time indicated as hours post-transfection (hpt). A) Cell growth kinetics and viability. B) Volumetric titer (VG/mL). C) Cell-specific viral yield (VG/cell). D) Functional titer (ETU/mL). E) Ratio between volumetric and functional titer (VG/ETU). n=1.